PHYSICAL REVIEW B VOLUME 25, NUMBER 3 1 FEBRUARY 1982

Mössbauer-effect studies on the magnetic properties of the Ni-Zn—ferrite system

T. M. Uen
Department of Physics, Tamkang University, Tamsui, Taiwan

P. K. Tseng
Department of Physics, National Taiwan University, Taipei, Taiwan
(Received 2 October 1980; revised manuscript received 11 June 1981)

The nickel-zinc—ferrite system $(Zn)_x(Ni)_{1-x}Fe_2O_4$, $0.20 \leq x \leq 0.75$, has been studied by means of the Mössbauer effect. The spectra taken at temperatures near and below the Néel temperature were explained by using the perturbation theory of relaxation line shapes for magnetically ordered systems. As the results of the fitting of the experimental spectrum, the average spins and the longitudinal relaxation rates of both *A*- and *B*-site ferric ions were obtained. Their temperature and zinc-content dependences were investigated and explained qualitatively. It was suggested that the dominant relaxation mechanism involves the modulation of the anisotropic part of the *A-O-B* superexchange interaction.

I. INTRODUCTION

The magnetic hyperfine structures of the nickel-zinc ferrites, $(Zn)_x(Ni)_{1-x}Fe_2O_4$, have been the subjects of many Mössbauer-effect studies for many years.[1–10] It was found that the Mössbauer spectra of this material at higher temperatures consisted of broad outer Zeeman lines and intense inner ones. The shapes of these spectra have been considered as an effect of the relaxation of the ionic spins in Ni-Zn ferrites.[6,9,10] It was also found that the linewidths of $(Zn)_{0.70}(Ni)_{0.30}Fe_2O_4$ at 77 K decreased significantly when an external magnetic field of 13.5 kG was applied.[6] The influence of such a weak field ($g\mu_B H_{ext} \sim 2$ K) on the linewidths is an important evidence of the presence of relaxation effects on the Mössbauer spectrum.

Under the assumption that the *A*- and *B*-site ferric ions have the same chemical environment, some researchers[9] fitted the spectra of several Ni-Zn ferrites with the relaxation line shapes of stochastic model.[11] Their calculated line shapes agreed qualitatively with the experimental ones when the temperature was not very close to the Néel temperature. When the temperatures was near the Néel temperature, they did not give the theoretical spectra and the relaxation times.

Although considerable advances in the understanding of the spin relaxation in Ni-Zn ferrites have resulted from the above-mentioned studies, there are still some interesting questions remaining to be answered. Most important among them are: (a) Is the relaxation rate of *A*-site ferric ions different from that of *B*-site ferric ions? (b) What are the temperature dependences of the relaxation rates, in particular, when the Néel temperature is approached? (c) What are the composition dependences of the relaxation rates? (d) What is the dominant relaxation mechanism in Ni-Zn ferrites? These questions need more careful and laborious studies to be answered. This paper reports our work on these questions.

II. EXPERIMENTAL

Our Ni-Zn ferrites were prepared with the usual ceramic method. Stoichiometric amounts of oxides were wet mixed, baked to dry at 90 °C, ground in a porcelain mortar, and pressed into pellets at a pressure of 9.5×10^3 psi with a hydraulic press. Then the pellets were sintered at 1200 ± 10 °C in a still-air atmosphere for 10 h with an electric furnace and thereafter cooled slowly in the furnace. X-ray-diffraction analyses[12] showed that all our samples were in the single phase of spinel structure. Chemical analyses[13] showed that the compositions were very close to the nominal ones.

The Mössbauer spectrometer used in this experiment was a Kankeleit-type[14] spectrometer in which the source of γ rays moved with a constant acceleration and the multichannel analyzer was operated in the time mode. The spectrometer was calibrated periodically with an α-Fe_2O_3 powder ab-

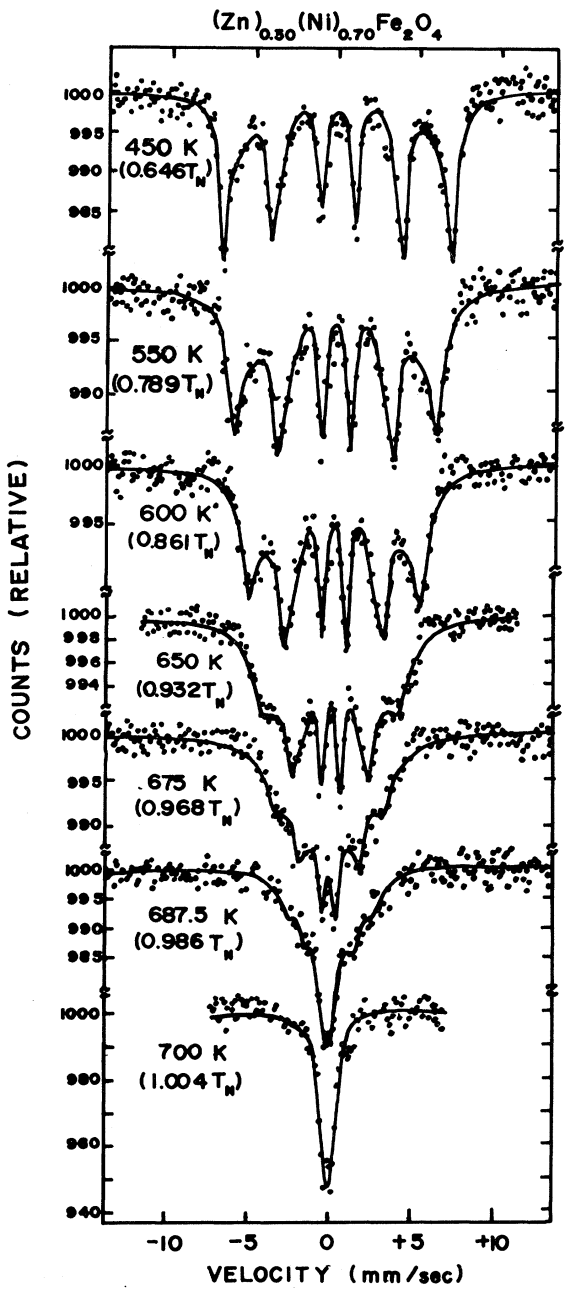

FIG. 1. Mössbauer spectra of $(Zn)_{0.30}(Ni)_{0.70}Fe_2O_4$. The solid curves are the best two-site fits.

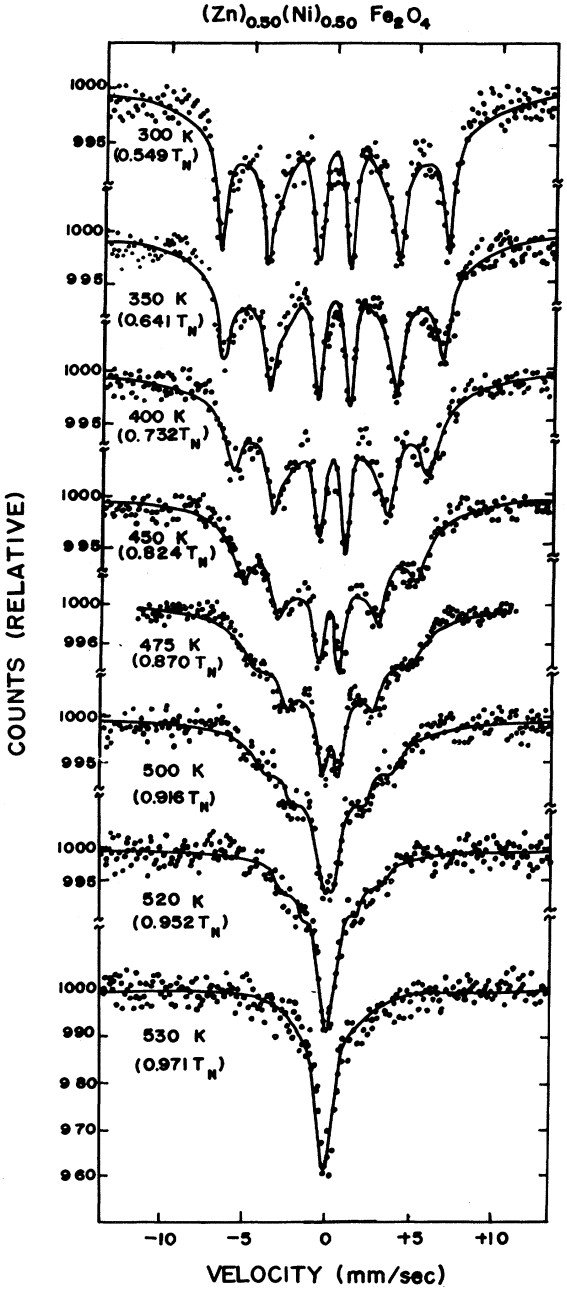

FIG. 2. Mössbauer spectra of $(Zn)_{0.50}(Ni)_{0.50}Fe_2O_4$. The solid curves are the best two-site fits.

sorber. The ferrite absorbers were about 15-mg/cm^2 thick. The temperatures of the absorbers were controlled to within $\pm 0.50\,^{\circ}C$ by a proportional controller with voltage feedback. The source of 14.4-keV γ rays was ^{57}Co in a palladium matrix. All spectra were obtained in transmission geometry and gamma rays were monitored with a proportional counter.

III. SPECTRA AND THEIR FITTINGS

Figures 1 and 2 show, respectively, the Mössbauer spectra of $(Zn)_{0.30}(Ni)_{0.70}Fe_2O_4$ and $(Zn)_{0.50}(Ni)_{0.50}Fe_2O_4$ at various temperatures. They are typical relaxation spectra of nickel-zinc ferrites. It is particularly interesting that the outmost pair of lines are the broadest ones while the innermost

pair are the narrowest. This feature is especially evident for the spectrum at 650 °K in Fig. 1. It is well known that the longitudinal relaxation of the ionic spin has such effects on the shape of Mössbauer spectrum.[15,16]

To explain the experimental spectra quantitatively and to extract the relaxation parameters, we fitted the spectra by using the perturbation theory developed by Levinson and Luban.[16] The longitudinal and transverse correlation functions of a ferric spin were written, respectively, as[17]

$$\langle \delta S_z(\tau)\delta S_z(0)\rangle = \langle (\delta S_z)^2\rangle \exp(-R_L|\tau|)\,,$$
$$\langle \delta S_x(\tau)\delta S_x(0)\rangle = \langle S_x^2\rangle \exp(-R_T|\tau|)\,, \tag{1}$$

where the angular bracket denotes a thermal average,

$$\delta S_z(t) = S_z(t) - \langle S_z\rangle,$$
$$\delta S_x(t) = S_x(t) - \langle S_x\rangle = S_x(t)\,,$$

R_L and R_T are the longitudinal and transverse relaxation rates, respectively. Using Eq. (1) and the result of Levingson and Luban [Eq. (29) in Ref. 16], the line-shape function for the particular Mössbauer transition from $|M_g\rangle$ state to $|M_e\rangle$ state is given by

$$I_{M_gM_e}(\omega) = \sum_{P=-1}^{+1} |(M_g|I^{-P}|M_e)|^2 \exp(C_L A_{M_gM_e}/R_L^2 + C_T B_{M_gM_e}/R_T^2)$$
$$\times \int_{-\infty}^{\infty} dt \exp\{it[\omega + (\omega_g^z M_g - \omega_e^z M_e)]$$
$$+ [-(\Gamma_{M_gM_e} + C_L A_{M_gM_e}/R_L + C_T B_{M_gM_e}/R_T)|t|]\}$$
$$\times \exp\{-[(C_L A_{M_gM_e}/R_L^2)\exp(-R_L|t|) + (C_T B_{M_gM_e}/R_T^2\exp(-R_T|t|)]\}\,, \tag{2}$$

where $\hbar\omega$ is the transition energy, I is the intrinsic angular momentum operator associated with the transition, and $\Gamma_{M_gM_e}$ is the half-width in the absence of relaxation broadening. Other constants are defined as follows:

$$C_L = \langle (\delta S_z)^2\rangle,\quad C_T = \langle S_x^2\rangle,\quad \hbar\omega_g^z = A_g^z\langle S_z\rangle,$$
$$\hbar\omega_e^z = A_e^z\langle S_z\rangle,\quad A_{M_gM_e} = (A_g^z M_g - A_e^z M_e)^2\,,$$
$$B_{M_gM_e} = (A_g^x)^2(I_g^2 + I_g - M_g^2) + (A_e^x)^2(I_e^2 + I_e - M_e^2)\,.$$

Also, A_g^i and A_e^i $(i = x,y,z)$ are the hyperfine constants when the nucleus is in the ground and excited states, respectively.

Since the ferric ions occupied both tetrahedral A- and octahedral B-site in Ni-Zn ferrites,[8] the ^{57}Fe Mössbauer spectra should consist of two sets of relaxed Zeeman patterns with different relaxation parameters. Therefore, the fitting function was written as

$$I(\omega) = \sum_{A,B}\sum_{M_g,M_e} I_{M_gM_e}(\omega)\,. \tag{3}$$

In order to avoid the difficulty of too many parameters in the fitting function, we made the following assumptions: (a) $\Gamma_{M_gM_e}$, A_g^i, and A_e^i for each site can be obtained from other experiments (refer to Table I). (b) R_T's are so large that the transversal terms in Eq. (2) are very small compared to the longitudinal ones and can be neglected.[18] (c) The thermal averages in Eq. (2) can be calculated from the Boltzmann factor p of the successive ionic Zeeman levels. For example, the average spin of the A-site ferric ions is given by

$$\langle S_z\rangle_A = \frac{-5p_A^5 - 3p_A^4 - p_A^3 + p_A^2 + 3p_A + 5}{2(p_A^5 + p_A^4 + p_A^3 + p_A^2 + p_A + 1)}\,. \tag{4}$$

Under these assumptions, the number of relaxation parameters in our least-square fitting shrinked to four. The relaxation parameters were the longitudinal relaxation rates, R_{LA} and R_{LB}, and the Boltzmann factors, p_A and p_B.

In Figs. 3(a)–3(d) we show the best (two-sites) fits to the experimental spectra of $(Zn)_{0.60}(Ni)_{0.40}Fe_2O_4$ at 300 K, and $(Zn)_{0.50}(Ni)_{0.50}Fe_2O_4$ at 300, 400, and 475 K, respectively. We notice that the agreements are satisfactory. For comparison, we also show in the same figures the best single-site fits in which the chemical environments of A- and

TABLE I. Values of fixed parameters.

x	H_A (kOe)	H_B (kOe)	Γ_{upper} (mm/sec)	Γ_{lower}[a] (mm/sec)	$\frac{Area(A)}{Area(B)}$ $\left[=\frac{1-x}{1+x}\right]$	Remark
0.20	510	531	0.22	0.11	0.667	b
0.30	511	530	0.24	0.11	0.538	b
0.40	512	519	0.215	0.11	0.429	b
0.50	505	521	0.275	0.11	0.333	b
0.54	505	519	0.245	0.11	0.299	c
0.57	505	518	0.25	0.11	0.274	c
0.60	505	517	0.25	0.11	0.250	b
0.65	505	515	0.21	0.11	0.212	c
0.70	505	512	0.175	0.11	0.176	b
0.75	506	513	0.155	0.11	0.143	c

[a]$\Gamma_{lower}=0.11$ mm/sec is the resolution of our spectrometer.
[b]The hyperfine fields are quoted from Ref. 8 and Γ_{upper} is the half-width of peaks 1 and 6 for A-site Fe^{3+} at 7 K reported in Ref. 8.
[c]H_A, H_B, and Γ_{upper} are obtained through the linear interpolations of the related data reported in Ref. 8.

B-site ferric ions were considered as identical. To inspect the thickness effects on the fitting, the spectrum of a thickened absorber of $(Zn)_{0.60}(Ni)_{0.40}Fe_2O_4$ at 300 K was taken with an expanded velocity scale and then fitted with the two-site line shape. The result is shown in Fig. 3(e). It was found that the fitting is also satisfactory. In Tables II–V we list the Boltzmann factors and logitudinal relaxation rates obtained from our fittings. The error in each entry of this table is the square root of the related diagonal element of the error matrix of the least-squares fitting.

IV. AVERAGE SPINS OF FERRIC IONS

In Fig. 4 we show the temperature dependences of the average spins $\langle \bar{S}_z \rangle$'s (reduced to the value 1 at 0 K) of the A- and B-site ferric ions for several Ni-Zn ferrites. In the same figure, we also show the average spin determined by Bhargava and Iyengar using the Mössbauer effect[9] and the reduced sublattice magnetizations $\bar{m}$'s determined by Satya Murthy *et al.* using the neutron diffraction method[19] for the ferrites with $x=0.50$ and 0.75.

The average spin of Bhargava and Iyengar in Fig. 4 was obtained using the single-site fitting of the spectra. Therefore, it is reasonable that their data falls between our $\langle \bar{S}_z \rangle_A$ and $\langle \bar{S}_z \rangle_B$ for both $x=0.50$ and 0.75.

According to the cation distribution $(Zn_xFe_{1-x})(Ni_{1-x}Fe_{1+x})O_4$, only ferric ions contribute to the A-site sublattice magnetization while both ferric and nickel ions contribute to the B-site sublattice magnetization. Consequently, only A-site average spin should be compared directly with A-site sublattice magnetization. As shown in Fig. 4, the values of our $\langle \bar{S}_z \rangle_A$ agree with those of $\bar{m}_A$ for $(Zn)_{0.50}(Ni)_{0.50}Fe_2O_4$. For $(Zn)_{0.75}(Ni)_{0.25}Fe_2O_4$, the values of $\bar{m}_A$ differ considerably from those of our $\langle \bar{S}_z \rangle_A$.

It is noticed in Fig. 4 and Tables II–V that $\langle \bar{S}_z \rangle_A$ is considerably greater than $\langle \bar{S}_z \rangle_B$ for all the ten samples being studied. This result can be explained as following: Ni-Zn ferrites are ferrimagnetic spinels in which the intersublattice A-O-B superexchange interaction is stronger than either of the two intrasublattice interactions.[20] On the average, each A-site ferric ion has $6(1-x)$ Ni^{2+} and $6(1+x)$ Fe^{3+} ions on the B sites as its nearest magnetic neighbors. On the other hand, each B-site ferric ion has only $6(1-x)$ Fe^{3+} ions on the A sites as its nearest magnetic neighbors. The larger number of A-O-B superexchange bonds for each A-site ferric ion results in a stronger effective field acting at the A-site Fe^{3+} and therefore results in the greater $\langle \bar{S}_z \rangle_A$ at any given temperature below the Néel temperature.

The discussions in the last paragraph lead also to the result that $\langle \bar{S}_z \rangle_B$ decreases with increasing

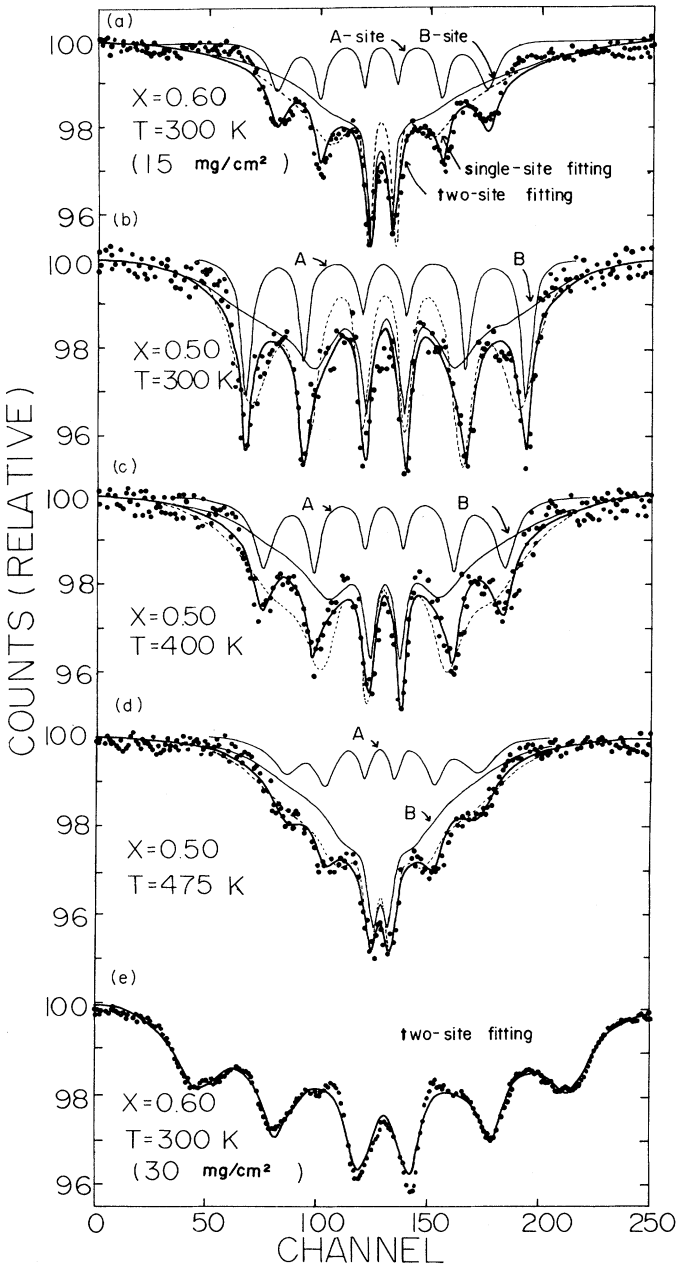

FIG. 3. Best single-site and two-site fits to the spectra of: (a) $(Zn)_{0.60}(Ni)_{0.40}Fe_2O_4$ at 300 K, (b) $(Zn)_{0.50}(Ni)_{0.50}Fe_2O_4$ at 300 K, (c) $(Zn)_{0.50}(Ni)_{0.50}Fe_2O_4$ at 400 K, and (d) $(Zn)_{0.50}(Ni)_{0.50}Fe_2O_4$ at 475 K, (e) $(Zn)_{0.60}(Ni)_{0.40}Fe_2O_4$ with thickness 30 mg/cm^2 at 300 K. Note that the velocity scale is different from that of (a).

zinc content while $\langle \bar{S}_z \rangle_A$ is relatively independent of the zinc content. This feature is clearly observed in Fig. 5. In Fig. 5 we show the zinc-content dependences of $\langle \bar{S}_z \rangle_A$ and $\langle \bar{S}_z \rangle_B$ at $T/T_N = 0.78$. We notice that both $\langle \bar{S}_z \rangle_A$ and $\langle \bar{S}_z \rangle_B$ decrease when the zinc content increases though $\langle \bar{S}_z \rangle_A$ is relatively independent of the zinc content. The decrease of $\langle \bar{S}_z \rangle_A$ with increasing zinc content means that the $Fe_A^{3+}-O^{2-}-Ni_B^{2+}$ superexchange interaction is stronger than the $Fe_A^{3+}-O^{2-}-Fe_B^{3+}$ interaction. This result agrees with that of Morel.[4]

TABLE II. Results of data analyses for $(Zn)_{0.20}(Ni)_{0.80}Fe_2O_4$ and $(Zn)_{0.30}(Ni)_{0.70}Fe_2O_4$ with different Γ's.

		$p_A(10^{-3})$		$p_B(10^{-3})$		R_{LA} (10^6 sec^{-1})		R_{LB} (10^6 sec^{-1})	
x	T (K)	$\Gamma=0.11$	0.22	0.11	0.22	0.11	0.22	0.11	0.22 mm/sec
	600	411± 2	411±2	511± 3	503± 4	1250±140	2800±800	430± 40	500± 60
	650	494± 2	496±3	591± 4	581± 5	1130±130	1800±400	470± 50	510± 70
	700	587± 2	589±3	694± 3	681± 5	980± 90	1300±200	490± 40	530± 50
	712.5	615± 2	617±2	723± 2	716± 4	1040± 90	1500±200	620± 40	690± 60
0.20	719	625± 2	631±3	736± 3	721± 4	800± 60	1000±100	500± 50	520± 40
	726	652± 3	658±4	778± 3	763± 5	720± 60	800±100	490± 30	510± 50
	740	702± 3	708±4	828± 4	820± 6	880± 80	1100±100	400± 40	350± 40
	750	764± 5	766±6	918± 6	966±13	700±100	1100±200	290± 60	330± 60
	755	778±10	738±9	913± 9	941±13	600±200	1000±300	320± 80	500± 100
	760	800± 5	797±7	966±10	972±10	1200±200	1700±400	3500±600	25 000±22 000
		$\Gamma=0.11$	0.24	0.11	0.24	0.11	0.24	0.11	0.24 mm/sec
	500	350± 2	355± 3	465±5	445± 6	790± 90	1900± 600	230± 20	230± 30
	550	389± 2	389± 3	528±3	512± 5	670± 60	1100± 200	240± 20	270± 20
	600	501± 2	504± 3	626±3	610± 4	820± 60	1200± 200	310± 20	380± 30
0.30	650	601± 2	609± 4	729±3	707± 5	670± 50	800± 100	360± 20	360± 30
	667.5	640± 3	643± 5	784±2	765± 5	670± 50	700± 90	430± 20	410± 30
	687.5	765± 5	763± 6	909±4	931± 7	870±160	1500± 400	470± 60	600±100
	690.5	766±11	747±15	922±8	949±12	600±200	900± 400	450±100	640±170
	694	783± 7	772± 8	951±4	965± 7	1400±400	2500±1100	1100±200	1500±400

V. LONGITUDINAL RELAXATION RATES OF FERRIC SPINS

The typical temperature dependences of the longitudinal relaxation rates are shown in Figs. 6 and 7. We also show in Fig. 6 the single-site relaxation rates of $(Zn)_{0.50}(Ni)_{0.50}Fe_2O_4$ and $(Zn)_{0.75}(Ni)_{0.25}Fe_2O_4$ determined by Bhargava and Iyengar.[9] For $(Zn)_{0.50}(Ni)_{0.50}Fe_2O_4$, their relaxation rate agrees with our R_{LA}. However, for $(Zn)_{0.75}(Ni)_{0.25}Fe_2O_4$ their result differs considerably from ours when the temperature is high. The difference is believed to be due to the difference between the samples used.

Magnon-magnon and magnon-phonon scattering precesses are responsible for the longitudinal and transverse relaxations of the spins in Ni-Zn ferrites. Because the longitudinal relaxation rate is the relaxation rate of the total number of magnons,[21] only those scattering processes in which the number of magnons changed contribute to the longitudinal relaxation rate. The most important scattering processes are the three-magnon processes in which a magnon is created or absorbed and the two-magnon—one-phonon processes in which two magnons are combined into a phonon or a phonon is split into two magnons.[22,23] The three-magnon processes are related directly to the magnetic anisotropy energy, whilst the two-magnon—one-phonon processes just mentioned are caused by the dependence of the anisotropy energy on the deformation of the crystal.[22,23,24]

We notice that the longitudinal relaxation is induced by the magnetocrystalline anisotropy of the material. Three interactions are responsible for the magnetocrystalline anisotropy energy: the single-ion anisotropy, the dipole-dipole interaction, and the anisotropic part of the exchange interaction. The single-ion anisotropy arises from the effect of the crystal field on the energy level of the single ion and thus contributes only to the magnon-phonon processes. The dipole-dipole interaction and the anisotropic part of the exchange interaction, however, contribute to both magnon-magnon and magnon-phonon processes.

For the Ni-Zn ferrites, all single-ion anisotropy

TABLE III. Results of data analyses for $(Zn)_{0.40}(Ni)_{0.60}Fe_2O_4$, $(Zn)_{0.50}(Ni)_{0.50}Fe_2O_4$, and $(Zn)_{0.54}(Ni)_{0.46}Fe_2O_4$ with different Γ's.

		$p_A(10^{-3})$		$p_B(10^{-3})$		R_{LA} (10^6 sec^{-1})		R_{LB} (10^6sec^{-1})	
x	T (K)	Γ=0.11	0.215	0.11	0.215	0.11	0.215	0.11	0.215 mm/sec
0.40	400	306±3	309± 4	460±7	437± 8	700±100	1300± 400	170± 20	180± 20
	450	359±3	359± 3	517±6	504± 7	660± 80	1300± 300	180± 20	200± 20
	500	456±4	449± 4	589±8	576± 9	520± 60	700± 100	120± 10	160± 20
	550	530±2	530± 2	700±3	686± 4	580± 30	750± 60	210± 9	240± 10
	575	604±4	606± 5	780±5	762± 6	540± 60	680± 90	180± 20	210± 20
	600	693±8	706±10	861±5	880±11	430± 70	500± 100	200± 30	200± 30
	610	732±9	727± 9	901±5	931± 8	500±100	900± 200	340± 50	430± 60
	620	806±4	804± 4	952±2	961± 2	2700±700	8000±5000	1600±200	2800±600
		Γ=0.11	0.275	0.11	0.275	0.11	0.275	0.11	0.275 mm/sec
0.50	300	285± 2	278± 2	519±14	443± 7	290± 20	1500±600	43± 1	82± 8
	350	339± 3	323± 4	610±24	447± 7	240± 15	660±100	44± 1	89± 8
	400	429± 3	412± 4	659±13	575± 7	300± 20	640± 80	56± 2	110± 10
	450	533± 4	495± 5	801±15	675± 7	290± 25	660± 80	62± 2	140± 10
	475	579± 3	563± 4	809± 4	758± 4	350± 20	580± 50	88± 3	150± 10
	500	621± 5	628± 7	837± 5	849± 7	410± 50	740±130	130±10	190± 20
	520	708±11	718±10	882± 7	938±18	470±140	1200±400	220±50	330± 50
	530	723±11	723±10	924± 5	959±10	770±300	2100±700	560±90	860±170
		Γ=0.11	0.245	0.11	0.245	0.11	0.245	0.11	0.245 mm/sec
0.54	300	327± 3	308± 4	549±18	472± 7	310± 30	1000± 200	46± 1	110± 10
	350	408± 4	386± 4	643±18	557± 8	350± 30	800± 100	53± 2	100± 10
	400	478± 4	470± 5	737±10	682± 8	400± 40	800± 100	75± 4	110± 10
	450	612± 6	611± 8	819± 8	805±11	480± 70	700± 100	108± 9	140± 20
	475	642±14	659±13	872± 9	906±20	300± 80	400± 200	150± 20	190± 30
	490	720±23	689±26	909± 7	950±13	400± 200	700± 400	400±100	700± 200
	500	778± 7	774± 7	948± 2	958± 3	2400±1000	10000± 7000	2100±400	5000±2000

(SIA) energy comes from the ferric ions and can be described by the Hamiltonian[25,26]:

$$H_{\mathrm{SIA}} = \tfrac{1}{6}A_{\mathrm{Fe}}[\,S_x^4+S_y^4+S_z^4 - \tfrac{1}{5}S(S+1)(3S^2+3S+1)]\,. \tag{5}$$

The constant A_{Fe} in the last equation is a measure of the strength of the interaction between the ferric ion and the crystal field. It has been derived from the anisotropy constants for Ni-Zn ferrites by van Gronenou and Schulkes[27]:

$$A_{\mathrm{Fe}}^{A} = -1.6\times10^{-2}\,, \qquad A_{\mathrm{Fe}}^{B} = +2.7\times10^{-2} \tag{6}$$

in cm^{-1}. It is noticed in Eq. (6) that the magnitude of A_{Fe} of the B-site ferric ion is considerably greater than that of the A-site ferric ion. If the single-ion anisotropy plays the dominant role in the longitudinal relaxation, this feature will lead to the result $R_{LB} > R_{LA}$. Since experimentally $R_{LA} > R_{LB}$, we exclude the possibility that the single-ion anisotropy plays the dominant role in the longitudinal relaxation.

Considering only the isotropic exchange and dipole-dipole interactions, Kaganov and Tsukernik[22,23] found that the contribution R_3 of the three-magnon processes and the contribution R_{21} of the two-magnon—one-phonon processes to the longitudinal relaxation rate are given, respectively, by

TABLE IV. Results of data analyses for $(Zn)_{0.57}(Ni)_{0.43}Fe_2O_4$, $(Zn)_{0.60}(Ni)_{0.40}Fe_2O_4$ $(Zn)_{0.65}(Ni)_{0.35}Fe_2O_4$ with different Γ's.

		$p_A(10^{-3})$		$p_B(10^{-3})$		R_{LA} (10^6 sec^{-1})		R_{LB} (10^6 sec^{-1})	
x	T (K)	Γ=0.11	0.25	0.11	0.25	0.11	0.25	0.11	0.25 mm/sec
	200	160± 5	162± 5	439±13	398±10	110± 10	250± 50	36± 1	41± 2
	250	285± 5	284± 5	549±21	484±14	200± 10	380± 70	43± 2	50± 4
	300	354± 3	347± 3	622±12	541± 7	270± 20	540± 60	51± 1	67± 4
0.57	350	447± 4	435± 4	721±10	664± 9	330± 30	620± 80	66± 2	85± 6
	400	568± 8	543± 9	815± 9	804±12	340± 50	500± 100	96± 6	130± 10
	425	634± 9	631±11	849± 9	867±18	500±100	700± 200	130± 10	140± 20
	450	705±13	700± 6	885± 7	935±13	600±200	2000±1000	250± 50	390± 80
	460	775± 7	744± 6	942± 3	952± 3	1700±600	3000±2000	1400±200	1500±300
		Γ=0.11	0.25	0.11	0.25	0.11	0.25	0.11	0.25 mm/sec
	200	238± 5	234± 5	480±10	447± 9	240± 30	800± 300	50± 3	75± 8
	250	328± 5	323± 4	646±18	571±10	230± 20	410± 60	51± 1	56± 3
	300	404± 3	397± 4	702± 8	651± 9	250± 20	410± 40	60± 1	68± 3
0.60	350	503± 5	496± 5	781± 6	774± 7	380± 40	610± 90	95± 4	115± 8
	375	596± 8	591±12	842± 7	850±12	420± 80	520± 130	130± 10	150± 20
	400	668±13	604±13	862± 9	900±10	180± 80	400± 200	170± 30	280± 50
	430	705±12	717±10	946± 3	961± 3	1400±700	5000±2000	1500±300	3000±1000
		Γ=0.11	0.21	0.11	0.21	0.11	0.21	0.11	0.21 mm/sec
	200	319± 6	317± 6	655±24	601±23	220± 30	350± 60	50± 2	52± 3
	250	429± 9	420± 9	714± 4	679±15	260± 40	390± 70	65± 3	74± 6
0.65	300	503± 8	495± 8	789± 6	780± 6	250± 30	360± 60	94± 4	120± 8
	320	564±10	564±11	833± 6	843± 8	290± 60	430± 100	130± 10	160± 15
	350	678± 8	678± 8	931± 4	931± 8	1100±600	1800± 700	600± 40	630± 80
	360	677± 7	680± 7	938± 2	947± 3	1600±500	2900±1600	1300±100	1300±200

TABLE V. Results of data analyses for $(Zn)_{0.70}(Ni)_{0.30}Fe_2O_4$ and $(Zn)_{0.75}(ni)_{0.25}Fe_2O_4$ with different Γ's.

		$p_A(10^{-3})$		$p_B(10^{-3})$		R_{LA} (10^6 sec^{-1})		R_{LB} (10^6 sec^{-1})	
x	T (K)	Γ=0.11	0.175	0.11	0.175	0.11	0.175	0.11	0.175 mm/sec
	100	302± 7	300± 7	623±13	569±13	160± 20	210± 30	43± 1	43± 1
	150	369± 7	359± 8	700±14	686±12	250± 30	330± 50	60± 3	62± 3
0.70	200	460±10	453±11	751±10	730±12	220± 30	290± 50	62± 3	67± 4
	250	568±13	538±25	855±10	856±10	180± 70	300± 100	100± 10	140± 20
	300	735± 9	723± 6	952± 2	958± 2	1900±900	6000±5000	2100±300	2600±400
		Γ=0.11	0.155	0.11	0.155	0.11	0.155	0.11	0.155 mm/sec
	100	471±30	467±20	815±10	810±10	100± 30	160± 50	76± 4	84± 5
	125	480±20	469±23	818± 9	814±10	150± 50	200± 70	88± 6	98± 8
	150	506±10	505±10	844± 8	843±10	600± 200	700± 200	120±10	130± 10
0.75	175	588±10	591±10	879± 6	886± 7	1100± 400	1500± 700	270±30	280± 40
	200	690± 8	688± 8	921± 6	933± 8	2600±1600	3900±3500	420±70	480± 80
	212.5	754±10	751±10	951± 3	954± 3	5000±4000	8000±7000	2500±500	3100±800

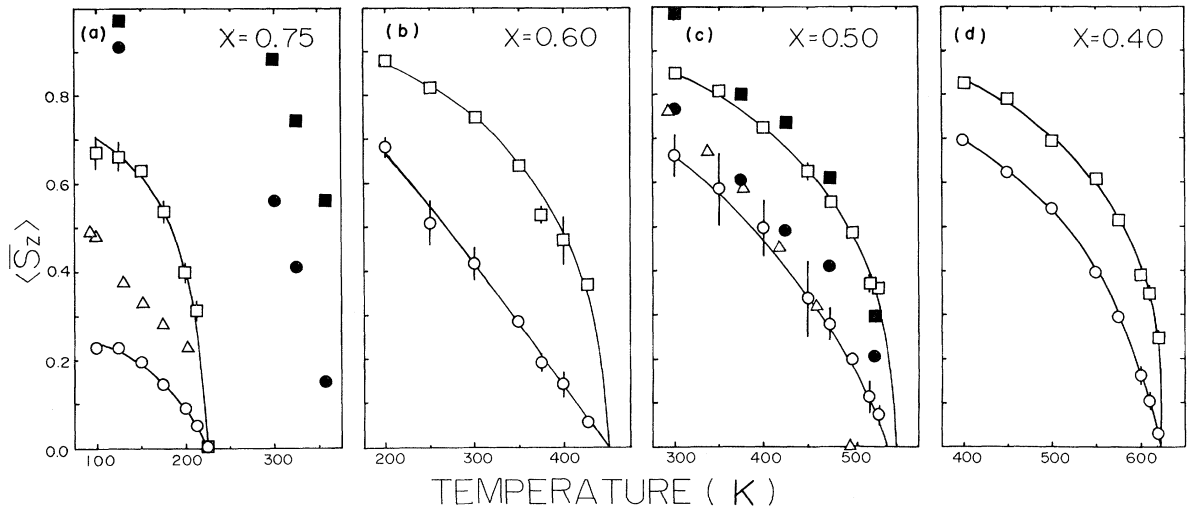

FIG. 4. Reduced average spins vs temperature of: (a) $(Zn)_{0.75}(Ni)_{0.25}Fe_2O_4$, (b) $(Zn)_{0.60}(Ni)_{0.40}Fe_2O_4$, (c) $(Zn)_{0.50}(Ni)_{0.50}Fe_2O_4$, and (d) $(Zn)_{0.40}(Ni)_{0.60}Fe_2O_4$. The symbols indicated in those graphs mean that (□): $\langle \bar{S}_z \rangle_A$, (○): $\langle \bar{S}_z \rangle_B$, (△): $\langle \bar{S}_z \rangle$ from Bhargava and Iyengar (Ref. 9), (■): $\bar{m}_A$ from Satya Murthy *et al.* (Ref. 18), (●): $\bar{m}_B$ from Satya Murthy *et al.* (Ref. 18).

$$R_3 \approx \begin{cases} 0.4(g^2\mu_B^2 M_0^2/2JS\hbar)(K_B T/2JS)^{1/2} \ln^2(g\mu_B H_{\text{eff}}/K_B T) & \text{when } g\mu_B H_{\text{eff}} << K_B T \quad (7a) \\ 1.4(g^2\mu_B^2 M_0^2/2JS\hbar)(g\mu_B H_{\text{eff}}/2JS)^{1/2} \exp(-g\mu_B H_{\text{eff}}/K_B T) & \text{when } g\mu_B H_{\text{eff}} >> K_B T \ , \quad (7b) \end{cases}$$

$$R_{21} \approx \begin{cases} (g\mu_B M_0/\hbar)(g\mu_B M_0/\rho\alpha^3 c_l^2)(T/\theta_D)^3 & \text{when } T << \theta_D^2/T_C \\ (\hbar/\rho\alpha^5)(g\mu_B M_0/K_B T_C)(T/T_C)^{1/2} & \text{when } T >> \theta_D^2/T_C \ . \end{cases} \quad (8)$$

In Eqs. (7) and (8), g, M_0, J, S, H_{eff}, ρ, α, c_l, θ_D, and T_C are, respectively, the g factor of the ion, the saturation magnetization of the sample, the isotropic exchange constant, the spin of the ion, the

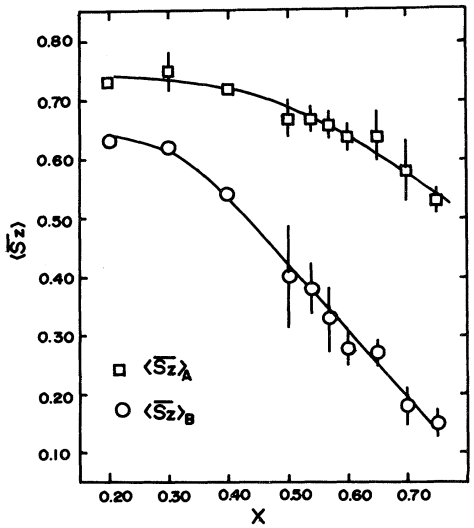

FIG. 5. $\langle \bar{S}_z \rangle_A$ and $\langle \bar{S}_z \rangle_B$ vs zinc content at $T/T_N = 0.78$.

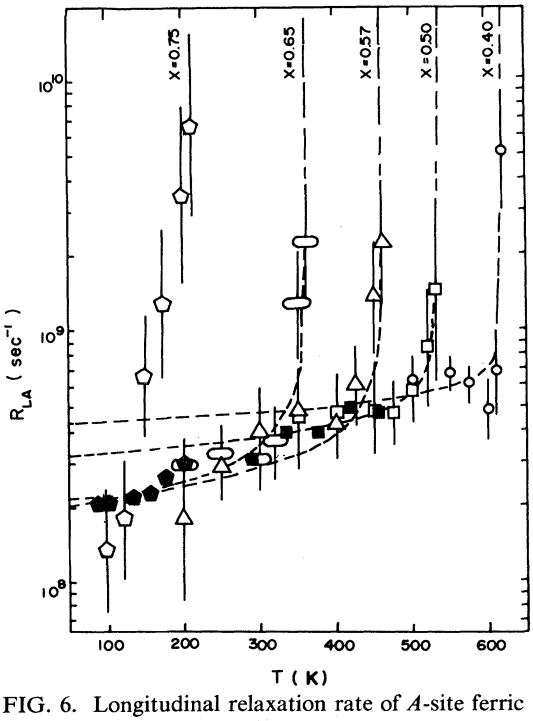

FIG. 6. Longitudinal relaxation rate of A-site ferric ion vs temperature. (⬟) and (■): $1/\tau$ from Bhargava and Iyengar (Ref. 9).

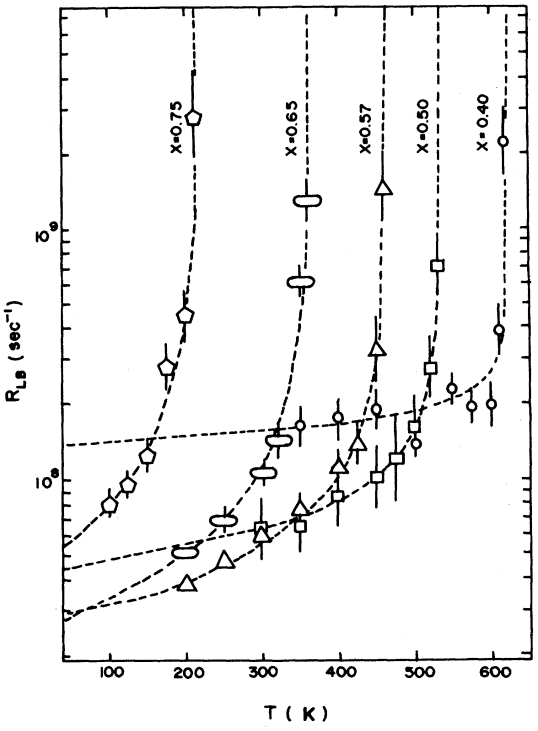

FIG. 7. Longitudinal relaxation rate of B-site ferric ion vs temperature.

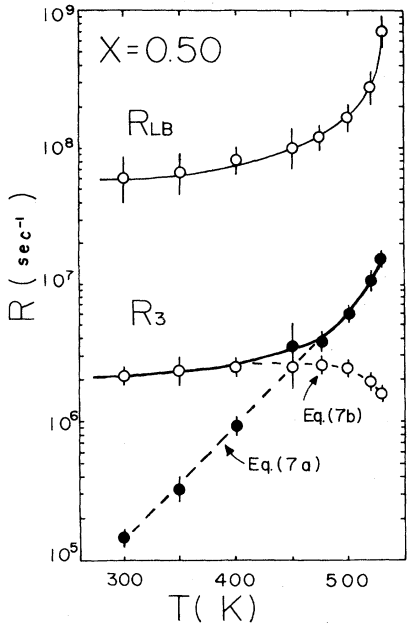

FIG. 8. Comparison of R_{LB} and R_3. In the R_3 curve, (●): value calculated with Eq. (7a), (○): value calculated with Eq. (7b).

effective magnetic field H_{eff} acting at the ion, the mass density of the sample, the lattice constant, the sound velocity, the Debye temperature, and the Curie or the Néel temperature. A very interesting feature is that R_3 diverges when the temperature approaches the critical temperature T_C at which H_{eff} vanishes, whereas R_{21} remains finite for all temperature. A quick estimation shows that $R_3 >> R_{21}$ when the temperature is not very low. For example, $R_3 = 3\times 10^7$ sec^{-1} while $R_{21} = 6\times 10^3$ sec^{-1} for $(Zn)_{0.50}(Ni)_{0.50}Fe_2O_4$ at 530 K. Deriving the effective magnetic field H_{eff} from the experimental value of the Boltzmann factor p by the equation

$$g\mu_B H_{\text{eff}}/K_B T = -\ln(p) , \tag{9}$$

we compared the experimental relaxation rate R_L with the three-magnon relaxation rate R_3 predicted by Eq. (7) (refer to Fig. 8). We found that, for each of the 10 samples being studied, there is a close parallelism between $R_L(T)$ and $R_3(T)$. The magnitude of $R_L(T)$ is however, larger than that of R_3 by one or two orders. We thus believe that when the temperature is not very near the Néel temperature (say, $T < 0.9T_N$), the dominant relaxation process is the three-magnon process induced by an interaction which is stronger than the dipole-dipole interaction by one or two orders. A possible candidate of this interaction is the pseudo-dipolar interaction, i.e., the anisotropic part of the superexchange interaction.

If the anisotropic part of the superexchange interaction plays the dominant role in the mechanism of longitudinal relaxation, then a ferric ion having more $A-O-B$ superexchange bonds relaxes more easily than a ferric ion having less $A-O-B$ bonds does. We thus expect that (a) $R_{LA} > R_{LB}$. (b) R_{LB} decreases when the zinc contest increases. (c) Compared with R_{LB}, R_{LA} is relatively independent of the zinc content. All these expected features are clearly observed in Figs. 6, 7, and 9. In Fig. 9 we show the zinc-content dependences of R_{LA} and R_{LB} at $p_A = p_B = 0.60$ (i.e., $K_B T = 3.9\mu_B H_{\text{eff}}$). The plotting of R_L's at a constant p, rather than at a constant T/T_N, is suggested by Eq. (7a) in which the strongest temperature dependence comes from the factor $\ln^2(g\mu_B H_{\text{eff}} / K_B T$ at high temperature. Based on the discussions in this paragraph and the last paragraph, we suggest that the dominant mechanism of longitudi-

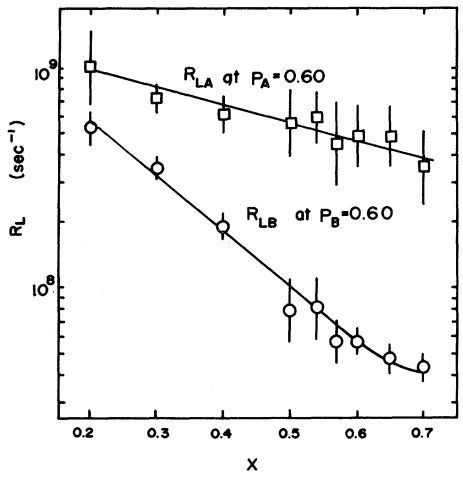

FIG. 9. Longitudinal relaxation rates at $p=0.60$ vs zinc content.

nal relaxation involves the anisotropic part of the superexchange interaction.

It is also noticed in Fig. 9 that R_{LA} decreases when the zinc content increases. When the zinc content increases, the decrease in the number of $Fe_A{}^{3+}-O^{2-}-Ni_B{}^{2+}$ bonds for an A-site ferric ion is accompanied by an increase of the same amount in the number of $Fe_A{}^{3+}-O^{2-}-Fe_B{}^{3+}$ bonds. The decrease of R_{LA} with increasing zinc content means that the relaxation channel for the A-site ferric ion through $Ni_B{}^{2+}$ is more effective than that through $Fe_B{}^{3+}$. This fact suggests that the anisotropic part of $Fe_A{}^{3+}-O^{2-}-Ni_B{}^{2+}$ interaction is stronger than that of $Fe_A{}^{3+}-O^{2-}-Fe_B{}^{3+}$ interaction.

VI. CONCLUSIONS

The nickel-zinc–ferrite system, $(Zn)_x(Ni)_{1-x}Fe_2O_4$, has been studied in detail by means of the Mössbauer effect. Mössbauer spectra of samples with various values of zinc content were taken at various temperatures near and below the Néel temperatures. As the results of the satisfactory fittings of the spectra with the perturbation theory of line shape,[16] the average spins and the longitudinal relaxation rates of both A- and B-site ferric ions were extracted. These quantities have been compared with previous results obtained by neutron diffraction[19] and the Mössbauer effect.[9] The temperature and zinc-content dependences of the average spins and the longitudinal relaxation rates have been discussed. Based on these investigations, we suggest that the dominant relaxation mechanism involves the anisotropic part of the A-O-B superexchange interaction.

ACKNOWLEDGMENTS

We are indebted to Professor U. Gonser, Professor S. S. Chen, and Professor C. L. Chien for their valuable discussions. Many thanks are also due to Professor H. S. Cheng for his help in the chemical analysis of our samples. We also are indebted to C. F. Ting, G. J. Jan, J. T. Lin, H. J. Ting, H. L. Chen, and S. M. Tsai for their help in the experimental work. Finally, one of us (T. M. U.) is grateful to the Sun Yet-sen foundation for the financial support during the past years. Also the experiment had been sponsored by National Science Council of the Republic of China.

[1]H. Abe, M. Matsuura, H. Yasuoka, A. Hirai, T. Hashi, and T. Fukuyama, J. Phys. Soc. Jpn. 18, 1400 (1963).

[2]V. I. Goldanskii, V. F. Belov, M. N. Devisheva, and V. A. Tsukhtanov, Sov. Phys. JETP 22, 1149 (1966) [Zh. Eksp. Teor. Fiz. 49, 168 (1965)].

[3]D. Kedem and T. Rothem, Phys. Rev. Lett. 18, 165 (1967).

[4]J. P. Morel, J. Phys. Chem. Solids 28, 629 (1967).

[5]G. A. Sawatzky, F. van der Woude, and A. H. Morrish, Phys. Rev. 187, 747 (1969).

[6]J. M. Daniels and A. Rosencwaig, Can. J. Phys. 48, 381 (1970).

[7]P. Raj and S. K. Kulshreshtha, Phys. Status Solidi A 4, 501 (1971).

[8]L. K. Leung, B. J. Evans, and A. H. Morrish, Phys. Rev. 8, 29 (1973).

[9]S. C. Bhargava and P. K. Iyengar, J. Phys. (Paris) 35, C6-669 (1974).

[10]T. M. Uen and P. K. Tseng, J. Phys. (Paris) 40, C2-261 (1979).

[11]For example, A. J. Dekker, in *Hyperfine Interaction*, edited by A. J. Freeman and R. B. Frankel (Academic, New York, 1967), Chap. S6.

[12]Performed kindly by the x-ray diffraction laboratory, Department of Geology, Taiwan University, Taipei.

[13]Performed kindly by C. G. Chen and Professor H. S. Cheng, Department of Chemistry, Tsing-hua University, Hsin-chu.

[14]E. Kankeleit, in *Mössbauer Effect Methodology*, edited by I. J. Gruverman (Plenum, New York, 1965), Vol. 2, p. 47.

[15]H. Wegener, Z. Phys. 186, 498 (1965).
[16]L. M. Levinson and M. Luban, Phys. Rev. 172, 268 (1968).
[17]L. D. Landau and E. M. Lifshitz, *Statistical Physics* (Addison-Wesley, London, 1974), Chap. 12.
[18]In magnetically condensed crystals, the most important scattering process which contributes to the transverse relaxation of magnetic moment is the four-magnon process induced by isotropic exchange interaction and thus the transverse relaxation rate is very high. See M. I. Kaganov, in *Ferromagnetic Resonance,* edited by S. V. Vonsovskii (Pergamon, Oxford, 1966), Chap. 4.
[19]N. S. Satya Murthy, M. G. Natera, S. I. Youssef, R. J. Begum, and C. M. Srivastava, Phys. Rev. 181, 969 (1969).
[20]C. Kittel, *Introduction to Solid State Physics* (Wiley, London, 1971), p. 550.
[21]C. W. Haas and H. B. Callen, in *Magnetism,* edited by G. T. Rado and H. Suhl (Academic, New York, 1963), Vol. 1, Chap. 10.
[22]M. I. Kaganov and V. M. Tsukernik, Sov. Phys. JETP 7, 1107 (1958) [Zh. Eksp. Teor. Fiz. 34, 1610 (1958)].
[23]M. I. Kaganov, in *Ferromagnetic Resonance,* edited by S. V. Vonsovskii (Pergamon, Oxford, 1966), Chap. 4.
[24]C. Kittel and E. Abrahams, Rev. Mod. Phys. 25, 114 (1953).
[25]J. Kanamori, in *Magnetism,* edited by G. T. Rado and H. Suhl (Academic, New York, 1963), Vol. 1, Chap. 4.
[26]S. Krupicka and K. Zaveta, in *Magnetic Oxides,* edited by D. J. Craik (Wiley, London, 1975), Chap. 5.
[27]A. Broese van Gronenou and J. A. Schulkes, J. Appl. Phys. 38, 1133 (1967).